International Journal of Thermal Sciences 131 (2018) 20–26

Contents lists available at ScienceDirect

International Journal of Thermal Sciences

journal homepage: www.elsevier.com/locate/ijts

Non-monotonously tuning thermal conductivity of graphite-nanosheets/paraffin composite by ultrasonic exfoliation

Bofeng Shang, Ruikang Wu, Jinyan Hu, Run Hu*, Xiaobing Luo**

State Key Laboratory of Coal Combustion, School of Energy and Power Engineering, Huazhong University of Science and Technology, Wuhan 430074, China

ARTICLE INFO

Keywords:
Ultrasonication exfoliation
Effective thermal conductivity
Graphite nanosheets
Non-monotonous variation
Phase change characteristics
Thermal storage performance

ABSTRACT

Organic phase change materials (PCMs) have drown continuous attentions over time due to their large latent heat and constant-temperature solid-liquid phase transition with promising applications in thermal energy storage. Nevertheless, they suffer from the relatively low intrinsic thermal conductivity. Filling the PCMs with graphite-nanosheets (GNs) by ultrasonic exfoliating could alleviate this problem, and GNs with longer ultrasonic exfoliation time is reported to possess larger effective thermal conductivity (ETC) monotonously. In this paper, we discover a non-monotonous variation of ETC for the first time, when enhancing the ETC of paraffin with ultrasonic exfoliated GNs. The mechanism behind this phenomenon is explained by the variation of GNs morphologies over time in the paraffin. Experimental results reveal that longer exfoliation time can increase the aspect ratio and ETC, but over a critical time, the bending stiffness of GNs decrease and the particles tend to be folded with increased interfacial thermal resistance and decreased ETC. The ETC as a function of ultrasonic time shows an obvious peak value at ~2 min, and the ETC could be increased from 0.3 to 3.0 W/(m·K) at GNs loading of 4 wt% with negligible effect on the phase change characteristics. In addition, the GNs/paraffin composite exhibits the quick thermal response and longer working time. The present non-monotonous discovery reveals the underlying mechanism and provides suggestions on the improvement of ultrasonic exfoliation process.

1. Introduction

Organic phase change materials (PCMs), such as paraffin, fatty acids and polyethylene glycols, have drown continuous attentions over time due to their large latent heat and wide range of melting/crystallization temperature of solid-liquid phase transitions with promising applications in thermal energy storage, electronic memory, and data storage [1–9]. Among these PCMs, paraffin is outstanding due to its appropriate melting point, large latent heat, high thermal stability, and low cost. However, the low thermal conductivity ($\kappa = \sim 0.4$ W/m·K) is the major drawback of paraffin in spite of many desirable properties, leading to low heat storage rates and limited application [10,11].

Filling the PCMs with high thermal conductivity particles is an effective scheme to enhance the effective thermal conductivity (ETC) of the composite and alleviate the problem. Traditional high thermal conductivity materials such as copper fins [12] and metal foams [13,14] offer increased ETC but are limited by manufacturing constraints and intrinsic thermal conductivity, and the foam structure has been proved to suppress the natural convection within the PCMs during the phase change process. Consequently, researchers have turned their attentions to high thermal conductivity carbon-based nanoparticles, such as carbon nanotubes [15,16], graphite-nanosheets (GNs) [17,18], and graphene [19,20]. Due to the low cost and relatively easy preparation, the GNs have been widely investigated as thermal enhancer in PCMs. Several groups proposed the liquid-phase ultrasonic exfoliation method to exfoliate expanded graphite (EG) into nanosheets with a thickness at nanoscale (~5–10 nm) [21–24]. Successful exfoliation requires to overcome the Van der Waals force between the adjacent layers of graphite. One effective and straightforward method to reduce the strength of Van der Waals attractions is liquid immersion. EG can be successfully exfoliated in liquid environments by exploiting ultrasound to extract individual layers [25]. During ultrasonication, the micrometer-sized bubbles or voids will be generated and burst in liquids due to pressure fluctuations, which give rise to shear forces to exfoliate the EG. After exfoliation, the inter-sheet attractive forces need to be overcame by the interaction between the GNs and the solvents. Solvents with surface tension of about 40 mJ/m^2 are appropriate since they minimize the interfacial tension between solvent and graphite, i.e. the force that minimizes the area of the surfaces in contact [25]. If the surface tension of the solvent is high, the particles tend to adhere to

* Corresponding author.
** Corresponding author.
E-mail addresses: hurun@hust.edu.cn (R. Hu), luoxb@hust.edu.cn (X. Luo).

https://doi.org/10.1016/j.ijthermalsci.2018.05.019
Received 30 January 2018; Received in revised form 20 April 2018; Accepted 12 May 2018

each other and aggregate together. Unfortunately, the majority of solvents with surface tension of 40 mJ/m^2 such as N-Methyl-2pyrrolidone (NMP ~ 40 mJ/m^2), N,N-dimethylformamide (DMF ~ 37.1 mJ/m^2), and ortho-dichlorobenzene (o-DCB ~ 37 mJ/m^2) are harmful to the human [17,25]. Thus an appropriate solvent is also important for the exfoliation of EG. On the other hand, the effect of the ultrasonic exfoliation time on the ETC of composite is still unclear. For instance, Haddon et al. [26] demonstrated that long-time exfoliation generates thinner GNs with larger aspect ratio (the ratio of in-plane size to out-of-plane size) and a higher ETC of the composite. However, Warzoha and Fleischer [27] came to an opposite conclusion. They claimed that the thinner GNs possess a lower bending stiffness and tend to be folded in the matrix. Such folding will give rise to a larger number of interfaces with more phonon boundary scattering, leading to larger interfacial thermal resistance and lower ETC. Similarly, Fang et al. [17] also claimed that smaller nanosheets possess higher specific surface area, phonons are easily scattered at the filler/PCM interfaces, resulting in a lower ETC. We feel confused for these diametrical conclusions, thus a further study of the ETC enhancement effect on exfoliation time is significantly needed.

In this paper, we used paraffin to exfoliate the graphite into nanosheets to prepare GNs/paraffin composite, including thermal expansion step, magnetic stirring step, and ultrasonication step. Different experimental specimens were prepared by controlling the exfoliation time from 0 min to 30 min. The ETC of each specimen was measured and the trend was analyzed. The phase change characteristics and the thermal storage performance of the GNs/paraffin composite was also assessed experimentally.

2. Materials preparation and characterizations

2.1. Materials preparation

Fig. 1a shows the process of preparing GNs/paraffin composite, which consists of thermal expansion, magnetic stirring, and ultrasonic exfoliation. Firstly, the natural graphite powders (XFnano, INC) were immersed in acid solution (20 vol% HNO_3 and 80 vol% H_2SO_4) to weaken the bonds between graphite layers. Secondly, the acid treated graphite powders were put into a microwave oven with an overall power of 800 W for 40 s to produce expanded graphite (EG). Thirdly, the EG was mixed with liquid paraffin ($C_{22}H_{46}$, RT44HC, Rubitherm) on a heating at 80 °C and fully stirred for 10 h via a magnetic stirring system. After that, the mixed liquid composites were ultrasonically exfoliated in a water bath at 80 °C, and the ultrasonic power was 650 W with frequency of 20–25 kHz. The paraffin not only acts as the matrix material, but also as the solvent in the ultrasonic exfoliation process to minimize the interfacial tension of the adjacent GNs layers, so as to avoid re-agglomeration. Fig. 1b shows schematic of the ultrasonic exfoliation system. We use a cell disrupter to produce ultrasonic wave to form small and energetic bubbles in the liquid medium. The bubbles burst instantaneously and release a huge amount of energy to exfoliate the EG. In order to confirm that the paraffin is able to exfoliate the EG, we measured the surface tension of the paraffin by Drop Shape Analyzer (DSA25, KRUSS). Results showed that the surface tension of paraffin is 34 mJ/m^2, approaching 40 mJ/m^2, indicating that paraffin can successfully exfoliate the EG into nanosheets. The ultrasonic exfoliation process ranges from 0 to 30 min to obtain GNs with different particle sizes. Finally, the prepared specimens were dried under vacuum at 80 °C to remove the bubbles.

2.2. Materials characterizations

Scanning electron microscope (SEM, Quanta 200, FEI) was performed to delineate the morphology of the GNs within paraffin at different mass loadings. All the specimens were pre-treated using the approaches described by Warzoha et al. [27]. Briefly, a brittle fracture was performed on each of the specimens in order to avoid significant displacement of GNs within the paraffin. Frictional forces from conventional cutting procedures could create a high temperature which would melt the paraffin in the vicinity of the cut and alter the paraffin distribution. Note that the GNs are coated in paraffin, thus their exact geometries cannot be directly extrapolated from these images. To obtain the diameter and thickness of the GNs, a phase separation process was conducted to avoid the paraffin masking the morphology of the GNs. Toluene solvent (Sinopharm Chemical Reagents Company, China) was adopted to dissolve the paraffin that covered on the surface of GNs, followed by the centrifugal treatment (8000 r/min, 5min), ultrasonic dispersion, filtration, and drying, and then the GNs powders were obtained. Atomic force microscopic (AFM, SPM9700, Shimadzu) and SEM tests were conducted to acquire the thickness and diameter of the GNs,

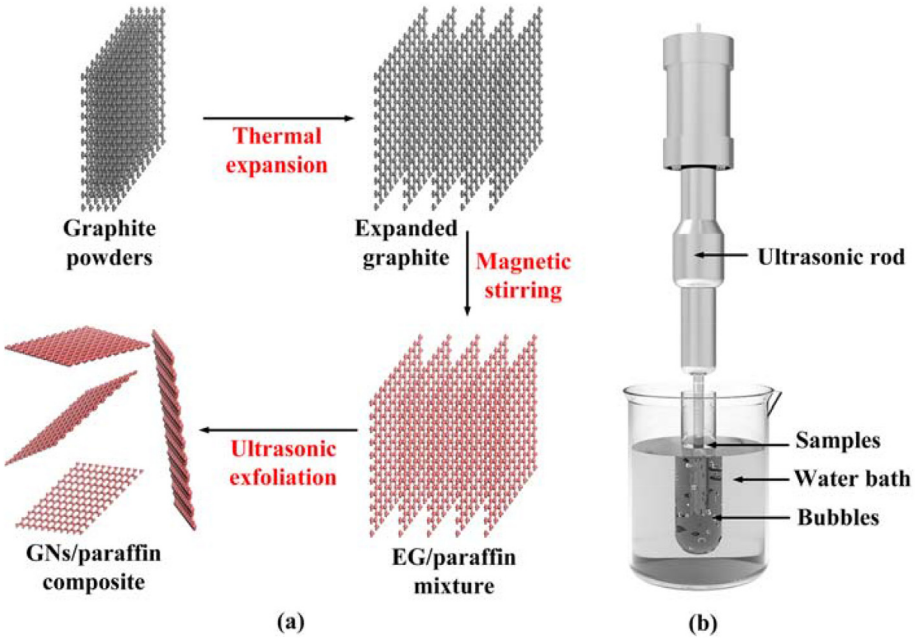

Fig. 1. (a) Process of preparing GNs/paraffn composite PCMs. (b) Schematic of ultrasonic exfoliation system.

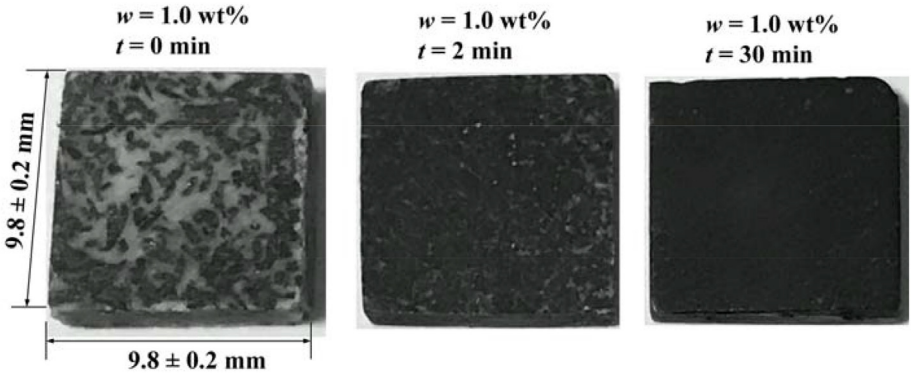

Fig. 2. Specimens prepared for thermal conductivity measurement by laser flashing method.

respectively. Differential scanning calorimeter (DSC, Diamond DSC, PerkinElmer) tests were conducted to measure the phase change characteristics including melting point, latent heat and specific heat. The test temperature ranges from 20 °C to 80 °C with a heating rate of 5 °C/min. The thermal conductivities of the samples were measured by laser flash method (NETZSCH-LFA467), and each of the tests have been repeated for five times to reduce the deviation error.

3. Results and discussion

3.1. Thermal conductivity of GNs/paraffin composite

Specimens with the mass fraction of GNs ranging from 0 to 4 wt% were prepared, and the ultrasonic exfoliation times were 0, 0.25, 0.5, 1, 2, 5, 15 and 30 min, respectively. Fig. 2 shows several specimens for thermal conductivity measurement. The dark parts represent the GNs, and the light parts represent paraffin. Initially, the worm-like EG with mass fraction of 1 wt% was added in paraffin. It can be observed that the EG was dispersed in paraffin and layering existing between the GNs and paraffin which cannot form a thermally conductive channel, resulting in an unapparent thermal enhancement effect. The layering phenomenon was significantly alleviated with 2-min ultrasonic exfoliation effect. As the ultrasonic exfoliation time increased, the particle sizes further decreased and the GNs were gradually uniform distributed in paraffin, resulting in the formation of compact network of GNs, which provided path for thermal conduction and improved the heat transfer rate accordingly.

Fig. 3 shows the thermal conductivity as a function of GNs loading

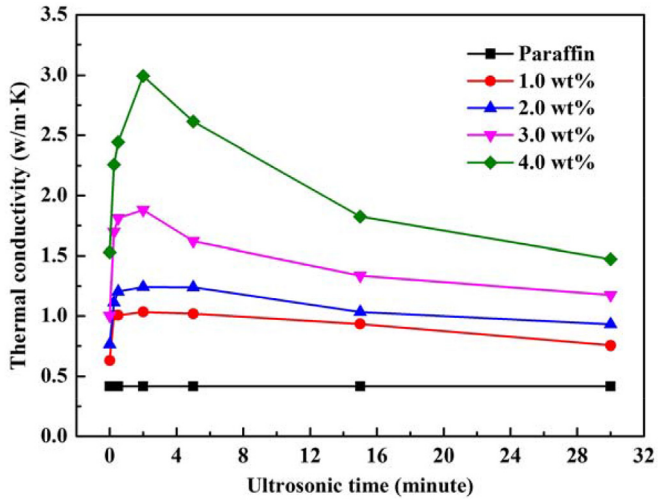

Fig. 3. Thermal conductivities of the composite as a function of ultrasonic time at different GNs loading.

at different ultrasonic time. It can be observed that the thermal conductivity of the GNs/paraffin composite is determined by ultrasonic time and GNs loading. The specimens possessed a higher thermal conductivity consistently as the GNs loading increased. The thermal conductivity was increased to be 3.0 W/(m·K) while the GNs loading was 4 wt%, revealing a significant thermal enhancement effect. In addition, an obvious peak value at 2 min for all studied GNs loadings is observed notably, rather than a monotonic trend reported in literature [17,26,27].

SEM and AFM tests were conducted to reveal the underlying physical mechanism of this nonlinear phenomenon. Fig. 4a presents an obvious worm-like structure which has a much larger out-of-plane size than in-plane size, resulting in a relatively low intrinsic thermal conductivity. After the ultrasonic exfoliation process, the worm-like EG was broken into individual graphite nanosheets as shown in Fig. 4b, resulting in a transition from 3-dimentional to 2-dimentional structure. The sheet structure possess a much higher in-plane size than out-of-plane size, which has been proved to have a much higher thermal conductivity than the original EG Ref. [26]. The increase of the filler's intrinsic thermal conductivity is the reason for the increase of the thermal conductivity of the composites, corresponding to the interval of 0–2 min in Fig. 3. In addition, the GNs were separated from paraffin to further reveal the sheets structure. Fig. 4d–f prove that the actual diameter of the GNs is about several micrometers, and the diameter decreases with the extended ultrasonic time. Individual nanosheets with average diameter of about 5.21 μm were obtained after 30-min ultrasonic exfoliation treatment, while for GNs with 2 min ultrasonic effect, the average diameter was 8.5 μm, and some were even as high as 13.5 μm. Moreover, the particles diameters were more uniform under longer ultrasonic time. AFM images in Fig. 4g and i reveal that the thickness of the particles were significantly reduced by the ultrasonic exfoliation effect. The thickness of GNs presents a similar tendency with the ultrasonic time, which is evaluated to be 5.48, 4.73 and 2.96 nm, respectively. However, the rigidity of the GNs decrease with the thickness, which may lead to bending and folding within the matrix as shown in Fig. 4c. These folding result in increased phonon boundary scattering at the interfaces. The stronger boundary scattering leads to an increase of interface thermal resistance and then decreases the intrinsic thermal conductivity of GNs. The negative influence of the interface thermal resistance surpassed the positive influence of the aspect ratio variation. Therefore, the thermal conductivity gradually decreases with the ultrasonic exfoliation time elapses. In conclusion, the thermal conductivity of the GNs/paraffin composite is found to be determined by both the positive effect of aspect ratio and negative influence of interface thermal resistance, and an optimal thermal conductivity of composite can be obtained with the variation of ultrasonic time.

Fig. 5 shows the comparison of the relative thermal conductivity enhancement with the GNs thermal enhanced composites reported in the literature. The enhancement ratio is defined as the ratio of thermal

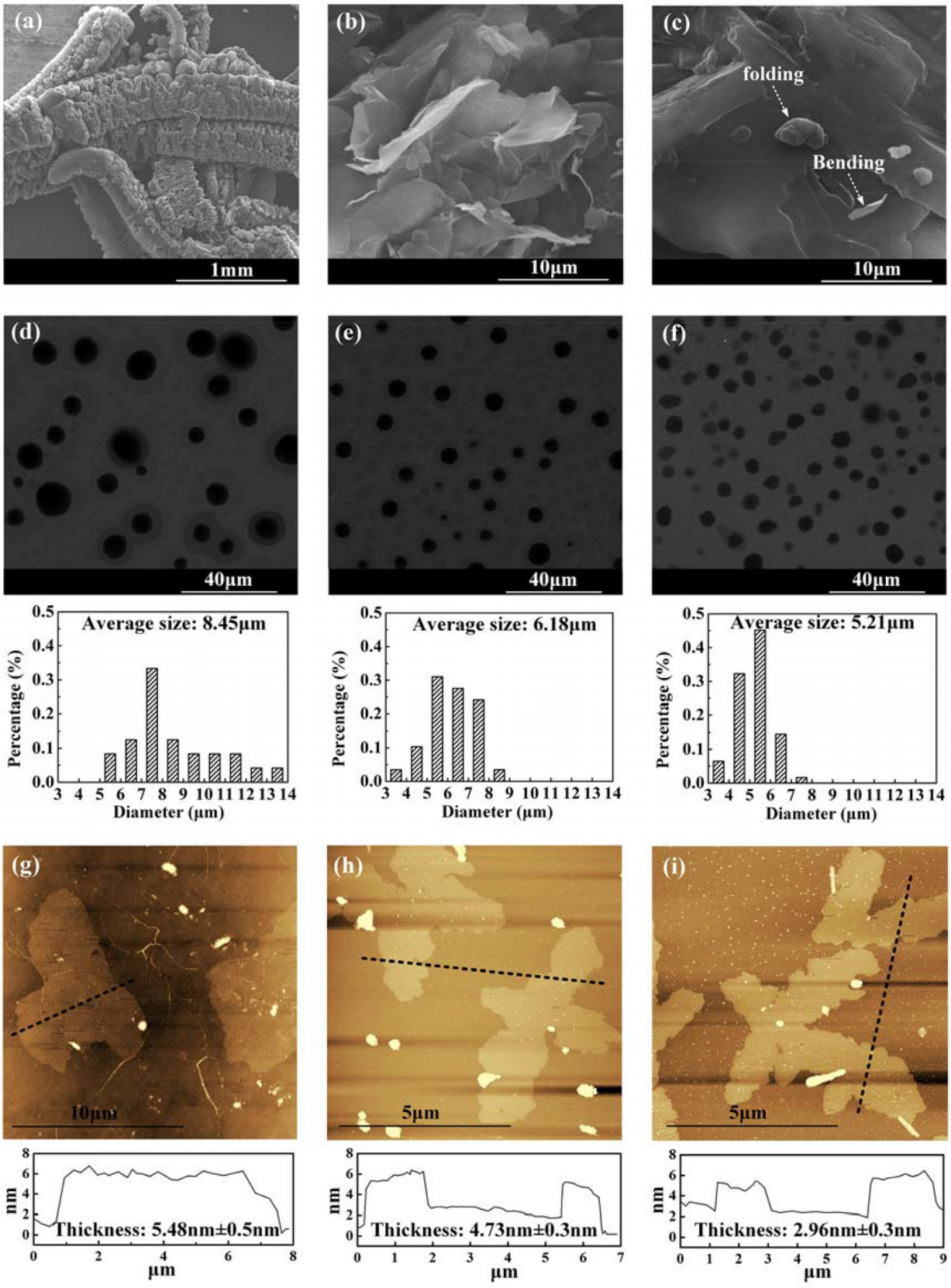

Fig. 4. (a–c) SEM images of EG, GNs/paraffin composites with ultrasound time of 2 min and 30 min, respectively. (d-f) SEM images of the GNs ultrasonic time of 2 min, 5 min and 30 min, respectively. (g-i) SEM images of the GNs ultrasonic time of 2 min, 5 min and 30 min, respectively.

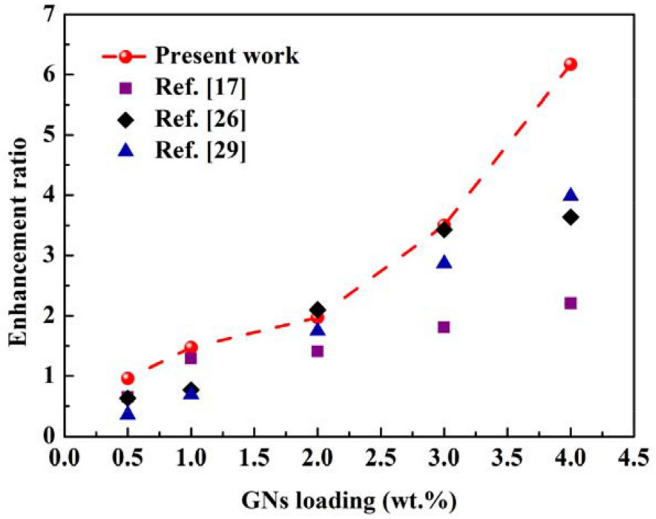

Fig. 5. Comparison of the relative thermal conductivity enhancements with the GNs thermal enhanced composites reported in the literature.

conductivity between the composites and the base material (paraffin in this paper). Results show that the enhancement ratio of thermal conductivity presented in our study are in a higher level, showing a promising potential in thermal energy storage systems.

3.2. Phase change characteristics of GNs/paraffin composite

Fig. 6a shows the DSC curves of pure paraffin, GNs/paraffin composites with the GNs loading of 0.5 wt% and 2.0 wt%, respectively. It was found that the DSC curves of all the test specimens are very similar, irrespective of the GNs loading. The onset, peak, and end represents the melting temperature, phase change temperature, and end temperature, respectively. The latent heat of each GNs/paraffin composite are calculated by integrating the heat transfer rate with temperature range over the endothermic peak. Fig. 6b presents the heat capacity of the samples at different temperature. It was found that the heat capacity of GNs/paraffin composites are similar with pure paraffin, indicating that the heat capacity was not affected by ultrasonic exfoliation effect. The heat capacity was about 2.0 J/g·K at room temperature, while it was surging to 67 J/g·K during phase change interval due to the large latent heat capacity. Fig. 6c illustrated the melting point temperature, phase-change temperature, and latent heat of the GNs/paraffin composites. The phase change temperatures of the specimens are within 46.23 ± 1 °C, which are very close to that of pure paraffin since no chemical reaction occurred between GNs and paraffin. Besides, the latent heat of pure paraffin was 241.44 J/g, and it was decreased to 227.26 J/g as the GNs loading increased to 4 wt%. Obviously, the latent heat is inversely proportional to the GNs loading, although the thermal conductivity increased with GNs loading. The latent heat reveals the intermolecular force or van der Waals force of paraffin, and the molecular potential energy in paraffin was increased during the phase change from solid to liquid by absorbing a large amount of energy. However, the volume expansion of paraffin was restricted by the presence of GNs, which increased the pressure in the pores and restricted the molecular heat transfer. As a result, the latent heat was reduced [28,29]. Furthermore, some of the paraffin was replaced by GNs, which further decreased the latent heat of the composite because of no phase change for GNs during the temperature range. Whereas these samples still maintain a latent heat capacity (> 225 J/g), showing a satisfying latent heat capacity. In general, the ultrasonic effect and the addition of GNs have negligible effect on the phase change characteristics of the composite, which will be beneficial for the application in thermal storage.

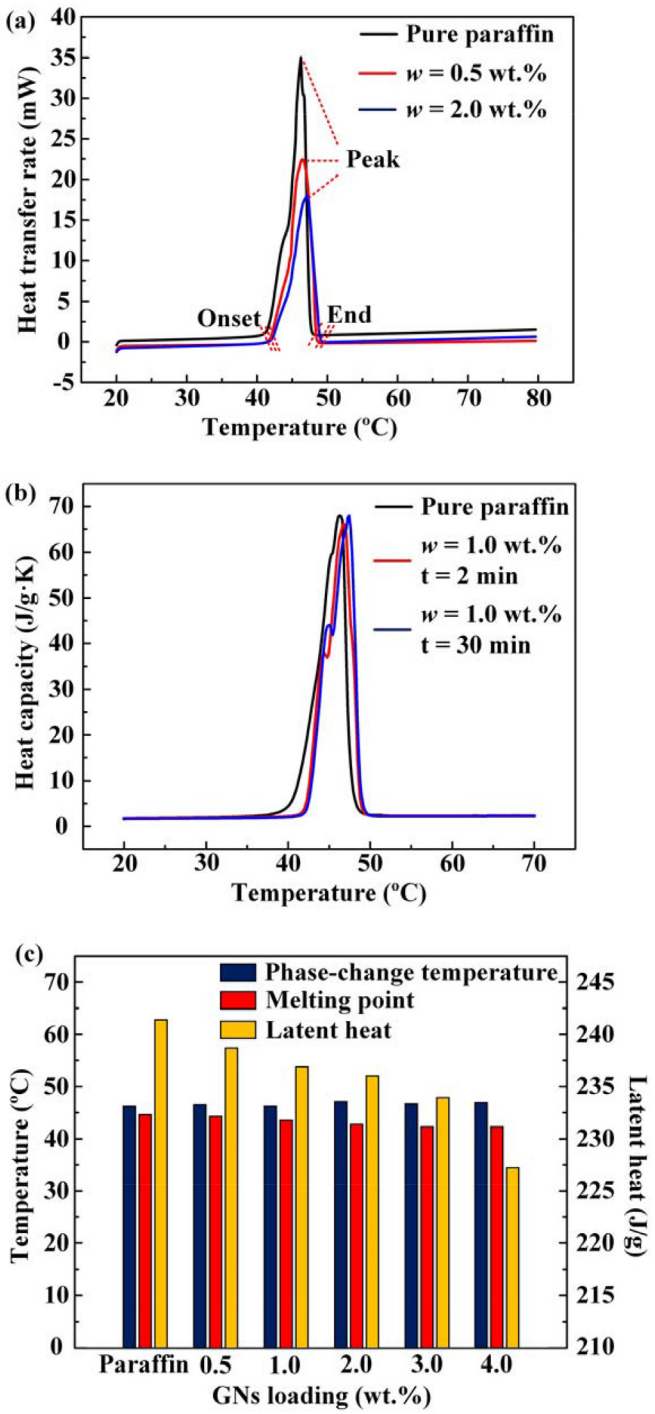

Fig. 6. (a) DSC curves of different specimens. (b) Heat capacity of different specimens. (c) Melting point, phase transition temperature, and latent heat of the GNs/paraffin composites.

3.3. Thermal storage performance of the GNs/paraffin composite

Fig. 7 shows the thermal storage performance of the GNs/paraffin composite. We prepared five different samples with the dimension of 100 mm × 100 mm × 30 mm, including pure paraffin (for comparison), EG/paraffin composite (for comparison) with EG loading of 1 wt % and 3 wt%, GNs/paraffin composite with GNs loading of 1 wt% and 3 wt%, respectively. The heating power was 30 W and the temperature threshold was set to be 80 °C. It reveals that the heat source temperature with GNs/paraffin composite is obviously lower than that of pure

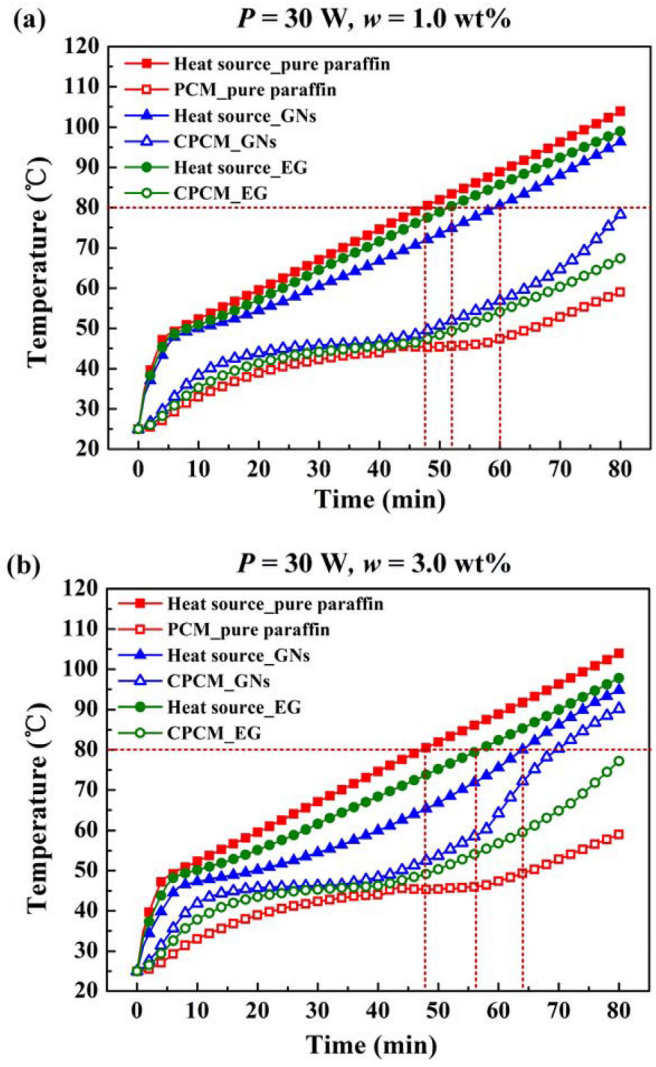

Fig. 7. The thermal storage performance of the GNs/paraffin composite. (a) P = 30 W, w = 1.0 wt%; (b) P = 30 W, w = 3.0 wt%.

paraffin and EG/paraffin composite due to its much higher thermal conductivity. The allowable working time was extended from 47 min to 60 min with 1.0 wt% GNs enhanced. The prolonging effect increase with the GNs loading, and the extension ratio of working time was increased to 36% with the GNs loading of 3.0 wt%. The results validates the quick thermal response and longer working time for the GNs/paraffin composite.

4. Conclusion

In summary, we prepare the GNs/paraffin composite by ultrasonic exfoliation method. The paraffin was adopted to exfoliate EG into nanosheets instead of those harmful solvents reported in literature. A non-monotonous variation of ETC was observed for the first time, and the thermal enhancement mechanism of GNs was revealed. The worm-like EG was exfoliated into GNs, which obviously has a larger aspect ratio and higher intrinsic thermal conductivity than the original EG, result in a higher ETC of the composite. The thickness of GNs decreased as ultrasonic exfoliation time prolonged further, leading to an increased number of interfaces due to GNs folding within the matrix and an increased phonon boundary scattering at the interfaces, resulting in a higher interface thermal resistance and a lower ETC. Besides, the thermal conductivity could be increased from 0.3 W/(m·K) to 3.0 W/(m·K) while the GNs loading is 4 wt%, with negligible effect on the phase change characteristics. The working time was extended by 36% with the GNs loading of 3 wt%, validating the quick thermal response and longer working time for the GNs/paraffin composite. Such non-monotonous discovery provides suggestions on the improvement of ultrasonic exfoliation process.

Acknowledgment

The authors would like to acknowledge the financial support by National Natural Science Foundation of China (51625601, 51576078, and 51606074), the Ministry of Science and Technology of the People's Republic of China (Project No. 2017YFE0100600), and the National Key R&D Program of China (Project No. 2016YFB0100901 and No. 2016YFB0400804). The authors would like to thank Ms. Wang for assistance with the DSC test and Mr. Yan for assistance with the AFM test.

References

[1] A. Sharma, V.V. Tyagi, C.R. Chen, D. Buddhi, Review on thermal energy storage with phase change material and applications, Renew Sust Energ Rev. 13 (2) (2009) 318–345.
[2] B.F. Shang, Y.P. Ma, R. Hu, C. Yuan, J.Y. Hu, X.B. Luo, Passive thermal management system for downhole electronics in harsh thermal environments, Appl Therm Eng 118 (2017) 593–599.
[3] X.B. Luo, R. Hu, S. Liu, K. Wang, Heat and fluid flow in high-power LED packaging and applications, Prog Energ Combust Sci. 56 (2016) 1–32.
[4] M. Li, Z.S. Wu, A review of intercalation composite phase change material: preparation, structure and properties, Renew Sust Energ Rev. 16 (4) (2012) 2094–2101.
[5] Y.P. Ma, R. Hu, X.J. Yu, B. Xie, X.B. Luo, A modified bidirectional thermal resistance model for junction and phosphor temperature estimation in phosphor-converted light-emitting diodes, Int J Heat Mass Tran 106 (2017) 1–6.
[6] G.D. Han, H.S. Li, J.C. Grossman, Optically-controlled long-term storage and release of thermal energy in phase-change materials, Nat Commun 8 (1) (2017) 1–10.
[7] R. Hu, S.L. Zhou, Y.L.I.D.Y. Lei, X.B. Luo, C.W. Qiu, Illusion thermotics, Adv Mater 1707237 (2018) 1–8.
[8] G. Atwood, Phase-change materials for electronic memories, Science 321 (5886) (2008) 210–211.
[9] F. Xiong, A.D. Liao, D. Estrada, E. Pop, Low-power switching of phase-change materials with carbon nanotube electrodes, Science 332 (6029) (2011) 568–570.
[10] L. Xia, P. Zhang, R.Z. Wang, Preparation and thermal characterization of expanded graphite/paraffin composite phase change material, Carbon 48 (9) (2010) 2538–2548.
[11] Z.G. Zhang, N. Zhang, J. Peng X.M Fang, X.N. Gao, Y.T. Fang, Preparation and thermal energy storage properties of paraffin/expanded graphite composite phase change material, Appl Energ 91 (1) (2012) 426–431.
[12] S.K. Saha, K. Srinivasan, P. Dutta, Studies on optimum distribution of fins in heat sinks filled with phase change materials, J Heat Tran 130 (3) (2008) 171–181.
[13] S. Mancin, A. Diani, L. Doretti, K. Hooman, L. Rossetto, Experimental analysis of phase change phenomenon of paraffin waxes embedded in copper foams, Int J Therm Sci 90 (2015) 79–89.
[14] W.Q. Li, H. Wan, H.J. Lou, Y.L. Fu, F. Qin, G.Q. He, Enhanced thermal management with microencapsulated phase change material particles infiltrated in cellular metal foam, Energy 127 (2017) 671–679.
[15] J.F. Wang, H.Q. Xie, Z. Xin, Thermal properties of paraffin based composites containing multi-walled carbon nanotubes, Thermochim Acta 488 (1) (2009) 39–42.
[16] X.G. Zhang, R.L. Wen, Z.H. Huang, C. Tang, Y.T. Huang, Y.A. Liu, et al., Enhancement of thermal conductivity by the introduction of carbon nanotubes as a filler in paraffin/expanded perlite form-stable phase-change materials, Energ. Buildings 149 (2017) 463–470.
[17] X. Fang, Q. Ding, L.Y. Li, K.S. Moon, C.P. Wong, Z.T. Yu, Tunable thermal conduction character of graphite-nanosheets-enhanced composite phase change materials via cooling rate control, Energy Convers Manage 103 (2015) 251–258.
[18] S. Kim, L.T. Drzal, High latent heat storage and high thermal conductive phase change materials using exfoliated graphite nanoplatelets, Sol. Energy Mat Sol C 93 (1) (2009) 136–142.
[19] B. Mortazavi, H.L. Yang, F. Mohebbi, G. Cuniberti, T. Rabczuk, Graphene or h-BN paraffin composite structures for the thermal management of Li-ion batteries: a multiscale investigation, Appl. Energy 202 (2017) 323–334.
[20] H. Babaei, P. Keblinski, J.M. Khodadadi, Thermal conductivity enhancement of paraffins by increasing the alignment of molecules through adding CNT/graphene, Int J Heat Mass Tran 58 (1–2) (2013) 209–216.
[21] L. Ma, J.J. Wang, A.M. Marconnet, A.C. Barbati, G.H. McKinley, W. Liu, et al., Viscosity and thermal conductivity of stable graphite suspensions near percolation, Nano Lett 15 (1) (2014) 127.
[22] J.L. Zeng, S.H. Zheng, S.B. Yu, F.R. Zhu, J. Gan, L. Zhu, et al., Preparation and thermal properties of palmitic acid/polyaniline/exfoliated graphite nanoplatelets formstable phase change materials, Appl. Energy 115 (2014) 603–609.
[23] K. Kalaitzidou, H. Fukushima, L.T. Drzal, Multifunctional polypropylene composites produced by incorporation of exfoliated graphite nanoplatelets, Carbon 45 (7)

(2007) 1446–1452.
[24] S. Wi, J. Seo, S.G. Jeong, S.J. Chang, Y. Kang, S. Kim, Thermal properties of shape-stabilized phase change materials using fatty acid ester and exfoliated graphite nanoplatelets for saving energy in buildings, Sol Energy Mat Sol C 143 (2015) 168–173.
[25] A. Ciesielski, P. Samorì, Graphene via sonication assisted liquid-phase exfoliation, Chem Soc Rev 43 (1) (2014) 381.
[26] A.P. Yu, P. Ramesh, M.E. Itkis, E. Bekyarova, R.C. Haddon, Graphite nanoplatelet-epoxy composite thermal interface materials, J Phys Chem C 111 (2007) 7565–7569.
[27] R.J. Warzoha, A.S. Fleischer, Effect of graphene layer thickness and mechanical compliance on interfacial heat flow and thermal conduction in solid-liquid phase change materials, ACS Appl Mater Inter 6 (15) (2014) 12868–12876.
[28] Z. Hashin, S. Shtrikman, A variational approach to the theory of the effective magnetic permeability of multiphase materials, J Appl Phys 33 (1962) 3125–3131.
[29] J.L. Xiang, L.T. Drzal, Investigation of exfoliated graphite nanoplatelets (x GnP) in improving thermal conductivity of paraffin wax-based phase change material, Solar Energy Mater Sol Cells 95 (2011) 1811–1818.